

Going with the flow: enhancing stochastic switching rates in multi-gyre systems

Christoffer R. Heckman*

U.S. Naval Research Laboratory
Code 6792
Plasma Physics Division
Nonlinear Dynamical Systems Section
Washington, DC 20375
Email: christoffer.heckman.ctr@nrl.navy.mil

M. Ani Hsieh

Scalable Autonomous Systems Lab
Mechanical Engineering & Mechanics
Drexel University
Philadelphia, PA 19104
Email: mhsieh1@drexel.edu

Ira B. Schwartz

U.S. Naval Research Laboratory
Code 6792
Plasma Physics Division
Nonlinear Dynamical Systems Section
Washington, DC 20375
Email address: ira.schwartz@nrl.navy.mil

A control strategy is employed that modifies the stochastic escape times from one basin of attraction to another in a model of a double-gyre flow. The system studied captures the behavior of a large class of fluid flows that circulate and have multiple almost invariant sets. In the presence of noise, a particle in one gyre may randomly switch to an adjacent gyre due to a rare large fluctuation. We show that large fluctuation theory may be applied for controlling autonomous agents in a stochastic environment, in fact leveraging the stochasticity to the advantage of switching between regions of interest and concluding that patterns may be broken or held over time as the result of noise. We demonstrate that a controller can effectively manipulate the probability of a large fluctuation; this demonstrates the potential of optimal control strategies that work in combination with the endemic stochastic environment. To demonstrate this, stochastic simulations and numerical continuation are employed to tie together experimental findings with predictions.

1 Introduction

Time-dependent and stochastic environments like the ocean feature a significant downside for sensor operation: under the influence of the flow, the sensors will escape from their monitoring region of interest with some finite probability. To prolong operational life-spans, it is therefore desirable to design mobile sensing control strategies subject to mini-

mizing the control effort. For environmental monitoring applications, typically one wishes to enable mobile sensors to either maintain their positions within a given region of interest or transition between regions to achieve more widespread sampling. For example, a common goal in a partitioned flow with multiple regions of interest is to either discourage or encourage transitions between them using an open-loop controller. In the former case, one strategy is to avoid high probability regions of transition; in the latter, only actuating an agent that happens into such a transition region will minimize effort while optimizing the probability to transition between regions of interest [1, 2]. However, this approach generally can be inefficient; oftentimes the controller does not take advantage of subtleties of the flow field itself to optimize across both control effort and transition probability.

Many systems are modeled with stochastic terms that represent uncertainties in model reduction [3,4], the variability in the time-dependent flow [1], and the fact that position is sensitive to small fluctuations in the flow itself [5]. Included in such systems is a wide class of circulatory flows, with “cells” of rotating current that are produced by eddies or vortices. These circulatory flows, commonly called gyres, are seen on length scales as small as blood flow in the atria of a heart [6] to circulation between terrestrial features in the ocean [7]. Many techniques exist to describe the qualitative aspects of such flows, including identifying Lagrangian coherent structures [8, 9, 10, 11], calculating finite-time Lyapunov exponents (FTLEs) to pinpoint persistent but trans-

lating manifolds [12], and large-scale modeling of the fluid systems themselves.

To study the many systems which are modeled with stochastic effects, mathematical methods have been developed to elucidate the effects of noise on dynamical behavior [13, 14, 15, 16, 1]. These methods accurately predict the expected dwell time of agents within an individual region of interest before transitioning and the likely paths for transitioning, including the most probable spatial exit points along the basin boundaries. Stochastic methods may be used to classify those phase space regions which are almost invariant [17] since deterministic basins of attraction no longer exist. Such sets are regions in which agents in the flow may remain for very long periods of time, but from which the agents will eventually escape.

In contrast to set-based controllers, we will develop a control approach that takes advantage of the flow governing the noise induced escape from a region of interest. Specifically, we wish to know the actual trajectory which has highest probability of escape. To design such a controller, we will study the effect of small noise on the transition times between two domains in a double-gyre flow. We will make use of the variational theory of large fluctuations as it applies to finding the *most probable*, or *optimal path* along which noise directs a particle to escape from an almost invariant region [18]. This optimal path and its corresponding switching rate will be used as a baseline in comparison with the switching rates for multi-gyre flows with control.

It is well-known that noise has a significant effect on deterministic dynamical systems. For example, consider a given initial state in the basin of attraction for a given attractor, which might be steady, periodic, or chaotic. Noise can cause the trajectory to cross the deterministic basin boundary and move into another, distinct basin of attraction [19, 20, 21, 22]. For sufficiently small noise, the dynamics are typically such that a particle first approaches a stable manifold which defines the basin boundary, and then approaches a saddle point on the basin boundary. Once the particle is near the saddle, basin boundary crossings may occur randomly where noise pushes the dynamics across the stable manifold after which point the particle is carried along the unstable direction away from the boundary. We note however that for large noise, such a crossing may be determined by the global manifold structure away from the saddle [23].

In the small noise limit, one can apply large fluctuation theory [24, 19, 20, 22], also known as large deviation theory used in white noise analysis [25, 24]. This approach enables one to determine the first passage times in a vector field with multiple basins of attraction, and has been applied to a variety of Hamiltonian and Lagrangian variational problems [26, 27, 28, 25, 29, 30, 31] outside of the context of control theory.

From a dynamical systems perspective, a subtlety to emphasize is that systems under the influence of noise no longer have deterministic paths that are governed by initial conditions. Instead, there is a probability density function that describes the most probable position of hypothetical particles within the flow. In stochastic systems that have mul-

tipole basins of attraction, there exist “most probable paths” for a hypothetical particle to transition between the two former stable motions (whether they be equilibria, limit cycles, or other dynamical behaviors). These transitional paths can be shown to be exponentially more likely to occur than others [24], and as a result even in systems that are under the influence of noise we can see through theory and experiment that these paths are strongly preferred for moving between adjoining basins. The presence of these paths enables us to exploit environmental forces to minimize control effort and therefore develop more energy efficient control strategies for small resource constrained mobile sensors operating in dynamic and uncertain environments. Large-fluctuation theory will enable us to identify these paths from a deterministic perspective when the dynamics of the system are more relevant than the noise intensity.

In this paper, we will show that large fluctuation theory may be applied for controlling multiple autonomous agents in a stochastic environment, in fact leveraging the stochasticity to the advantage of switching between basins and concluding that patterns may be held or broken over time as a result of noise [32]. The theory we develop will also be applicable to noise sources that are non-Gaussian due to the general nature of the formulation.

2 The model

Viewed from a kinematic perspective, a particle moving in a fluid-driven multi-gyre flow may be modeled as [33]

$$\dot{\mathbf{q}} = \mathbf{u} + \mathbf{F}(\mathbf{q}) + \boldsymbol{\eta}, \quad (1)$$

where $\mathbf{q} = (x, y)$; \mathbf{u} represents a control response, and $\boldsymbol{\eta}$ is a stochastic white noise term with mean zero and standard deviation $\sigma = \sqrt{2D}$ for a given noise intensity D . The delta-correlated noise is characterized by $\langle \eta_i(t) \rangle = 0$ and $\langle \eta_i(t) \eta_j(t') \rangle = 2D \delta_{ij} \delta(t - t')$. The component of the gyre flow $\mathbf{F} = (F_1, F_2)$ represents the deterministic, uncontrolled vector field given by

$$F_1 = -\pi A \sin(\pi x) \cos(\pi y/s) - \mu x \quad (2)$$

$$F_2 = \pi A \cos(\pi x) \sin(\pi y/s) - \mu y. \quad (3)$$

The parameter μ is a damping coefficient, s is a scaling dimension for the gyres, and A corresponds to the strength of the gyre flow. We note that undamped versions of the model were studied in [34], and that [16] also examined a forced, time-dependent version. A phase portrait of this system is provided in Figure 1.

The stochastic model will be used to quantify two situations in which noise plays an important role: the first will be an examination of agent escape times from the gyre without any control, and the second will examine the effect of small gyroscopic controls to advance or retard the escape times.

2.1 The uncontrolled deterministic flow

Consider the scenario without noise where $\boldsymbol{\eta} = 0$ and no controller is present. In this case, the system is completely determined by $\dot{\mathbf{q}} = \mathbf{F}(\mathbf{q})$, where \mathbf{F} is given in Eqs. (2),(3). The equilibria of the deterministic, uncontrolled flow without damping (i.e. when $\mu = 0$) are:

1. the origin $\mathbf{q}_0 = (0, 0)$, which is exact.
2. boundary equilibria: $(\pm 1, 0)$, $(0, \pm s)$, $(\pm 1, \pm s)$, $(\pm 1, \mp s)$.
3. gyre equilibria: $(\pm 1/2, \pm s/2)$, $(\pm 1/2, \mp s/2)$.

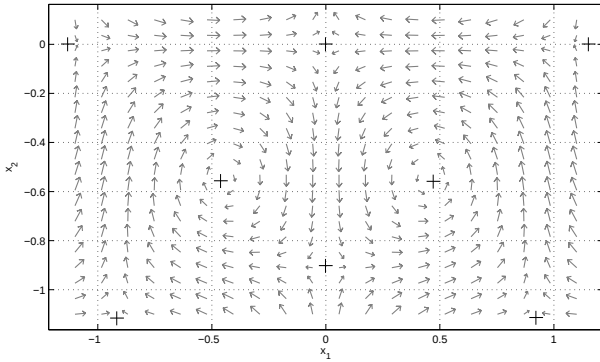


Fig. 1. Phase portrait of the two-gyre vector field with arrows denoting the flow direction and positions of equilibria marked by +. The parameters for this simulated flow are $A = 1$, $s = 1$ and $\mu = 1$.

Note that in Eqs. (2), (3), substituting $x \rightarrow -x$, $y \rightarrow -y$ results in the same equations of motion. Because of this symmetry, we will restrict our investigation to two adjacent gyres. Without loss of generality, we will consider switching between the two gyres which are centered at $\mathbf{q}_{A_l} = (-\frac{1}{2}, -\frac{s}{2})$ and $\mathbf{q}_{A_r} = (\frac{1}{2}, -\frac{s}{2})$, with the boundary point through which the switching occurs being $\mathbf{q}_B = (0, -s)$.

When $\mu \neq 0$, the positions of the equilibria \mathbf{q}_{A_l} , \mathbf{q}_{A_r} , and \mathbf{q}_B are perturbed. Although we use numerical approximations to calculate the coordinates of the equilibria, it is helpful to have an approximation so linearized stability determined from eigenvalues may be determined. Applying perturbation expansions for small μ to the gyre equilibria, their positions to second order in μ are:

$$x^* \approx \pm \frac{1}{2} \mp \frac{s}{2\pi^2 A} \mu \mp \frac{s}{2\pi^4 A^2} \mu^2 \quad (4)$$

$$y^* \approx \pm \frac{s}{2} \pm \frac{s}{2\pi^2 A} \mu \mp \frac{s^2}{2\pi^4 A^2} \mu^2. \quad (5)$$

Using this approximation, the real part of these eigenvalues to second order in μ is:

$$\Re(\chi^*) = -\mu + (s-1) \frac{\mu^2}{8A}. \quad (6)$$

This suggests that, when they exist, the gyre equilibria are stable for $\mu > 0$.

Both the gyre and boundary equilibria are born out of saddle-node bifurcations of the boundary equilibria and origin, respectively. Our following analysis is only relevant for the parameter subset in which all three types of equilibria exist and have these stability properties.

For small $\mu > 0$, the origin always has one stable and one unstable eigendirection. For the boundary equilibrium point at $(0, -s)$, we take the linearization using the small μ approximation and find that the real parts of the eigenvalues are:

$$\Re(\chi_1) = \pi^2 A - \mu - \frac{s^2 \mu^2}{2A} \quad \Re(\chi_2) = -\frac{\pi^2 A}{s} - \mu + \frac{s \mu^2}{2A}. \quad (7)$$

This implies that there also will always be one stable and one unstable eigendirection of this boundary equilibrium in the parameter subset in which we are interested.

To summarize the phase portrait of a single gyre and its boundary, the center of each gyre contains a stable focus and its basin of attraction is bounded by four saddle equilibria. Adjacent to this gyre on all sides are rotated and/or reflected replicas. Therefore, a system of two gyres sharing a boundary qualitatively resembles a potential field with two potential troughs separated by a peak. This illustration is helpful in considering stochastic trajectories that can cause a particle to switch its position from being in the basin of one gyre to that of another.

3 Noise-induced gyre escape

Under the influence of noise, the dynamical behavior of the system is determined by its stationary probability density. In particular, all equilibria are now peaks or troughs in a probability landscape describing where a particle is likely to be located. There are no orbits that are uniquely defined by a point along them, and as a corollary invariant manifolds (such as the gyre boundaries) cease to exist. Although there exist many paths that transport a particle from one gyre to another in the presence of small noise, there are “most likely paths” in the sense that they will lie along a local peak in the probability density. Such paths transitioning between gyre basins will pass from a local maximum of the distribution through a local minimum to a nearby local maximum. That is, the path of transition will begin at an attracting state, escape from the basin due to an effective force due to noise, and approach the other attracting state in a different basin. We characterize this transition by considering the most likely paths between the two states.

The probability of escape from an attractor under the influence of small white noise scales exponentially as

$$\mathcal{P}_{\boldsymbol{\eta}}(\mathbf{q}) = \exp(-\mathcal{R}(\mathbf{q}))/D, \quad (8)$$

where \mathcal{R} is the action [24]. Following the ideas in [25], we notice that for any given realization of noise, we have the approximate density scaling as $\exp(-\frac{1}{2} \int |\boldsymbol{\eta}|^2)$. If we continue the thinking of Feynman [24], then for any realization of noise we get the action of white noise defined in [25]. We take a general Hamiltonian approach which admits the formulation for escape induced by non-Gaussian noise [35].

3.1 Uncontrolled case

To put the problem into Hamiltonian formulation, we characterize the paths that require the minimum action of the dynamics and noise to cause the transition. In this approach, we use the vector field of Eq. 1 as a constraint. We may then use calculus of variations to accomplish the minimization. The action functional for the noise is:

$$\mathcal{R}[\mathbf{q}, \boldsymbol{\eta}, \boldsymbol{\lambda}] = \frac{1}{2} \int \boldsymbol{\eta}(t) \cdot \boldsymbol{\eta}(t) dt + \int \boldsymbol{\lambda} \cdot (\dot{\mathbf{q}} - \mathbf{F}(\mathbf{q}) - \boldsymbol{\eta}) dt. \quad (9)$$

When evaluating the action in Eq. 9, we compute $R = \min \mathcal{R}[\mathbf{q}, \boldsymbol{\eta}, \boldsymbol{\lambda}]$, where the minimum is taken over the functions $[\mathbf{q}, \boldsymbol{\eta}, \boldsymbol{\lambda}]$. Setting the first variation of the functional in Eq. (9) to zero will yield a system of differential equations that identify which solutions extremize the action in terms of the path and the minimum noise necessary to realize the path. This solution is the most probable path, even though it is rare and exists in the tail of the probability distribution for realizations of the noise.

The switching rate to switch from one region to another is directly proportional to the probability of observing the most likely noise profile to induce such a switch [18]; all other noise realizations are exponentially less likely. Therefore, the switching time may be approximated as:

$$T_S = b \exp\left(\frac{R}{D}\right) \quad (10)$$

where b is a prefactor which is determined through numerical simulation or experiment and $R = \min \mathcal{R}$. In order to calculate the switching time in Eq. (10), we must find the optimal trajectory and noise to induce a switch.

Computing the variational derivatives of the action and setting them to zero results in the following differential equations:

$$\dot{x} = F_1(x, y) + \lambda_1 \quad (11)$$

$$\dot{y} = F_2(x, y) + \lambda_2 \quad (12)$$

$$\dot{\lambda}_1 = -\frac{\partial F_1}{\partial x} \lambda_1 - \frac{\partial F_2}{\partial x} \lambda_2 \quad (13)$$

$$\dot{\lambda}_2 = -\frac{\partial F_1}{\partial y} \lambda_1 - \frac{\partial F_2}{\partial y} \lambda_2 \quad (14)$$

where λ_i represent the conjugate momenta to x, y .

The optimal path to transition between gyres is determined by the system above combined with a set of boundary conditions describing the gyre and boundary points. In particular the boundary conditions are $\mathbf{q}(t \rightarrow -\infty) = \mathbf{q}_{A_i}$ and $\mathbf{q}(t \rightarrow \infty) = \mathbf{q}_B$, with $\boldsymbol{\lambda}(t \pm \infty) = \mathbf{0}$.

Note that this is a deterministic system; its solution will dictate the optimal path to transition between the two gyres. Eqs. (11)–(14) contain equilibria at all locations in (x, y) as the system in Eqs. (2), (3) with the conjugate momenta equal to zero. Linearizing about the gyre equilibria in Eq. (11)–(14) and taking the real part of the eigenvalues of the gives

$$\Re(\chi_{1,2}) = -\mu + \frac{s-1}{8A} \mu^2$$

$$\Re(\chi_{3,4}) = \mu - \frac{s-1}{8A} \mu^2.$$

Note that both sets of eigenvalues share the same real part since they are complex conjugates; also, the equilibrium point has saddle stability. As for the origin, we have

$$\Re(\chi_{1,2}) = -(\pi^2 A + \mu) \quad \Re(\chi_{3,4}) = \frac{\pi^2 A}{s} - \mu.$$

The path connecting the equilibria is described as a two point boundary value problem governed by Eqs. (11)–(14) and the boundary conditions as explained above. Given the fact that the gyre attractor, \mathbf{q}_A , and the boundary saddle through which escape occurs, \mathbf{q}_B , are both saddle equilibria in the full set of equations of motion, finding the most optimal path mathematically requires identifying a heteroclinic orbit. To solve for the path numerically, we implement a numerical algorithm known as the IAMM [36]. We then employ numerical continuation using AUTO's HomCont [37] to increase the accuracy of the approximation and to study the behavior of the path using different parameter values.

It is important to note that the above exposition is analogous to the optimal trajectory generation problem where Eq. (9) is the objective function and Eqs. (2), (3) can be viewed as the vehicle kinematics. In this context, x and y are analogous to vehicle states and λ_i are the control inputs. Different from the canonical optimal control problem [38], λ_i represent the conjugate noise terms.

3.2 Controlled case

In the above analysis, we examined the eigenvalues of the equilibria in the expanded phase space without control. Now, we will consider the controlled system. The system equations are those in Eq. (1), including the gyre flow as given in Eqs. (2), (3), but now \mathbf{u} represents a gyroscopic control force. For brevity, define:

$$f_1 = -\pi A \sin(\pi x) \cos(\pi y/s)$$

$$f_2 = \pi A \cos(\pi x) \sin(\pi y/s).$$

Table 1. Comparison of calculated values of \mathcal{R} for two values of the control constant and the baseline case without control. The two nonzero values of c were arbitrarily chosen from a set of paths computed using continuation.

c	\mathcal{R}
0.0967	0.0977
0 (no control)	0.161
-0.314	0.379

We synthesize a controller that modifies the optimal path and therefore the transition probabilities. The controller we apply is:

$$\mathbf{u} = \boldsymbol{\omega} \times c \frac{[f_1, f_2, 0]}{\|[f_1, f_2, 0]\|}, \quad (15)$$

where c is a control parameter and $[f_1, f_2, 0]$ represents the conservative part of the vector field \mathbf{F} with an augmented trivial third dimension. Following Mallory et al. [2], we take the vector $\boldsymbol{\omega} = [0, 0, 1]^T$; i.e. it is a unit vector pointing into or out of the plane of the flow depending on the flow direction. The definition of \mathbf{u} imposes a controlled modification of the two-dimensional flow field.

Carrying out the cross product in Eq. (15) and plugging the final result into the vector field, we have:

$$\dot{x} = -c \frac{f_2}{\sqrt{f_1^2 + f_2^2}} + f_1 - \mu x + \eta_1 \quad (16)$$

$$\dot{y} = c \frac{f_1}{\sqrt{f_1^2 + f_2^2}} + f_2 - \mu y + \eta_2. \quad (17)$$

Recall that the action is logarithmically related to the probability of occurrence of escape. Since we are operating in the limit of small D , it guarantees that for a sufficiently small noise intensity, switching will only occur as a rare event and if switching should occur, it will be as a result of this particular event.

To compare switching rates in the controlled versus uncontrolled case, we choose two values of c —one positive and one negative—as examples for regimes in which the particle is meant to be ejected or contained from the present gyre respectively. The two values of the control constant and their corresponding values of the action are given in Table 1.

Note that as c is increased, the action \mathcal{R} decreases. Therefore, the particle is more likely to escape from one gyre to another with the controller turned on.

4 Simulation Results

We consider two methods to compare the theory developed in the previous section with numerical experiments: di-

rect comparison of probability density functions of numerically simulated paths that lead to switching with the theoretically predicted paths, and comparison of the mean first passage time (MFPT) from one gyre to another via simulation and that obtained using the predicted estimate in Eq. (10).

Numerical simulations were obtained via stochastic integration using an explicit Milstein method [39]. All simulations started with initial conditions at the center of the gyre \mathbf{q}_A , and were run until they crossed the line $x = 0$, at which point the particle's trajectory and the total time of the integration were recorded. Using these two measures, we are able to compare the anticipated MFPT and the path itself with expected results from large fluctuation theory. All stochastic simulations were run in batches of 3,000 trials.

In Figure 2, the optimal path to escape is shown for $c = 0$, whereas in Figure 3, the path is shown for $c = 0.0967$. The two-dimensional histograms over which these paths are imposed shows the stochastic simulations of paths that have passed to the adjacent gyre. Note that red indicates a higher incidence of occurrence and blue shows less occurrence. The full histories of these paths have been truncated and the results are shown on a logarithmic scale to accentuate the ridge of higher probability.

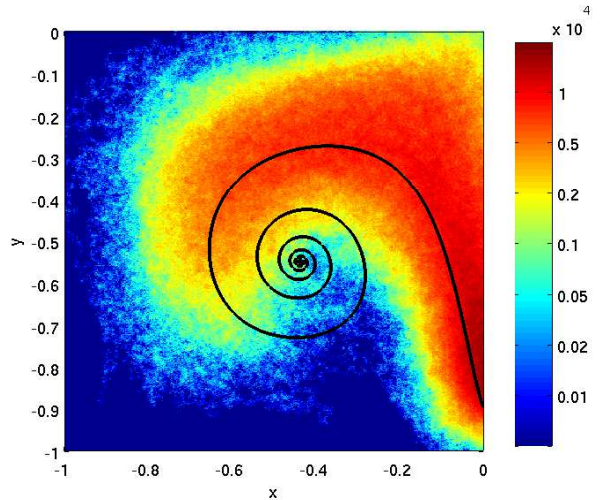


Fig. 2. Optimal switching path for $c = 0$ overlaid on a probability density function (pdf) of paths that have been stochastically integrated until transitioning out of the basin of attraction. The colormap represents an exponential scale of 3,000 sample paths with $D = 1/30$

Figure 4 shows a plot of the conjugate momenta versus time along the optimal path as computed using numerical continuation. This profile of the noise shows that it is optimally always acting to push the particle outward, strengthening as the distance from the center increases until it reaches the saddle point.

Finally, Figure 5 compares the MFPT of a particle via stochastic simulation and that expected using the theory.

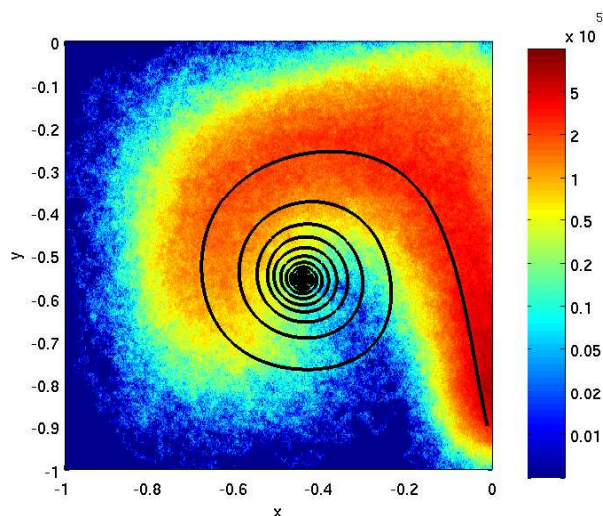


Fig. 3. Optimal switching path for $c \approx 0.1$ overlaid on a pdf of paths that have been stochastically integrated until transitioning out of the basin of attraction. Paths were generated by the same method as in Fig. 2

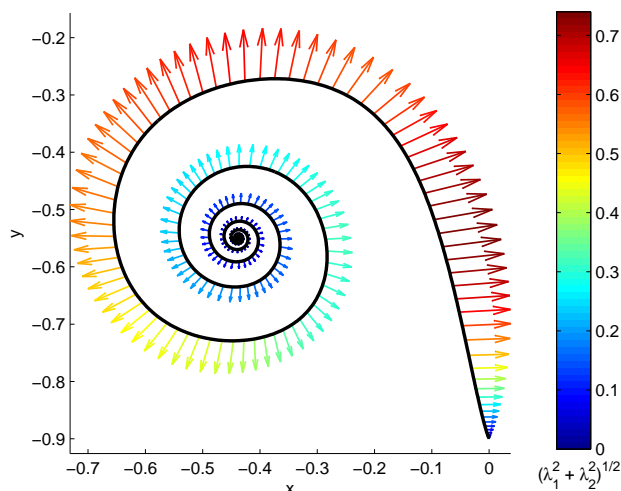


Fig. 4. The conjugate momenta along the optimal path as generated by AUTO for $c = 0$. The arrows indicate the direction in which the optimal noise is acting at the given point along the optimal path, and the color and length of the arrows indicate the magnitude of the noise.

5 Conclusions and Discussion

In this paper we have discussed a new approach to analyzing the control of systems under the influence of weak noise by utilizing a controller that manipulates the residence time of an agent switching between adjacent basins of attraction. Because of the stochasticity inherent to the dynamics of the flow, there will be a rare but non-negligible chance that an agent will inadvertently drift out of the region in which it should remain; this may be aided or abated by a controller that aims to maximize or minimize the mean first passage time between the basins. Both contexts are imper-

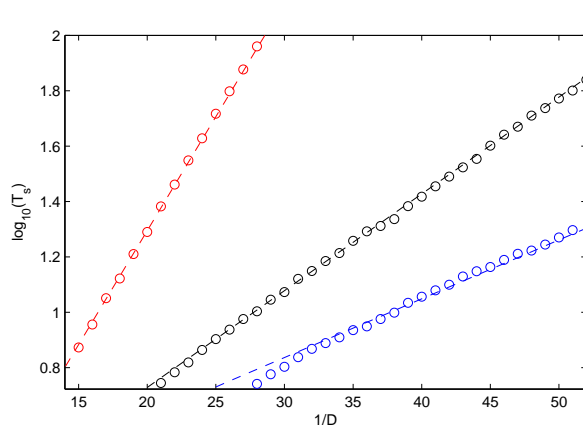


Fig. 5. Comparison of the MFPT as predicted by large-fluctuation theory (dashed lines) and computed from an average over many stochastic trials (points). Three regimes were examined: black represents no control, red represents $c \approx -0.31$ and blue represents $c \approx 0.1$

ative in many cases. In the example where there are many inexpensive, independently-acting vessels that are tasked to uniformly cover a domain composed of multiple basins of attraction, random redistribution of the vessels will occur via stochastic effects. It is advantageous in this example to choose a vessel that would be easier to propel into an adjacent cell, apply a weak controller that works in conjunction with noise to facilitate a transition, and on all the other vessels apply control so as to impede a transition. We have shown that with a simple, gyroscopic control approach this is a feasible approach.

To show that efficacy of this approach, we analyzed the mean first passage time from one basin to an adjacent one using a gyroscopic control strategy. Specifically, we showed there exists a logarithmic scaling of the mean escape times from one basin to another as a function of the noise in the environment. Such scalings persist without control, and the MFPT may be increased or decreased depending on the control settings. Even though the controller never changed the stability of the equilibrium point, there was a noticeable effect on the transition rate as witnessed in the stochastic simulations. We also showed that the logarithm of the transition rates need not be calculated using massive stochastic simulations, but rather can be approximated by using large fluctuation theory. This enables us to predict mean first-passage times and obtain an approximation for the reliability of the controller in a stochastic environment.

In deploying a fleet of many small minimally propelled vessels, one objective is to establish a given (possibly non-uniform) spatial distribution of buoys throughout the domain of interest. If the domain is similar to multi-gyre flows, then it may be necessary to make the buoys switch from one gyre to another if the density is too high in a particular region. Simulations were run for negative and positive c values in Eq. (15) in order to demonstrate that the controller can either maintain or change its gyre position. Since switching will always occur (albeit rarely) with no control imposed,

it is advantageous to decrease the likelihood of a random switch—and therefore applying the control with $c < 0$ will help maintain the status quo.

The results from both numerical simulations and large fluctuation theory confirm this hypothesis. Both approaches show that the MFPT for a particle is decreased for $c > 0$ and is increased for $c < 0$. That is, when the control is focused inward then the particle resides inside its original gyre for much longer than if the control is focused outward. Since in a truly stochastic environment there will always be unwanted transitions between basins of attraction, gyroscopic control has been shown to manipulate the transition rate so a targeted spatial distribution may be attained [2].

We will also note that in reference to Figures 2 and 3, while the paths near the gyre are difficult to resolve, the transition paths near the boundary point is in agreement with the optimal path predictions. By decreasing D we can more effectively resolve the sample histories and show agreement with the large-fluctuation prediction, but the computation time increases exponentially for small decreases in the noise intensity. The results we show display a trade-off between these factors, but it still captures the most salient feature of the analysis: there is a strong preference to approach the boundary point along a particular trajectory. This fact may be leveraged in the design of other controllers that might aim to expend effort to following along this trajectory and instigate a boundary crossing with minimal energy expenditure.

Another noteworthy result is that the optimal paths for $c > 0$ are more tightly wound than for $c = 0$; i.e. the path that contributes to the larger action in fact requires a very large fluctuation in order to cross into the adjacent basin. While at first this may be surprising, it may be explained by the qualitative action of the controller. Since for $c > 0$ the controller encourages leaving the center of the gyre, a series of more-likely smaller fluctuations (rather than a single very large one) will enable a particle to overcome the effective potential barrier and escape the basin.

These results have important implications for the design of controllers in the presence of noise. A vector field when influenced by stochastic effects retains many of the same dynamical behaviors of the original system, but there is the possibility for random switching events. With the knowledge of which paths are most likely to lead to a transition, we may pick our controller constants in order to minimize the MFPT. This is particularly important because it permits the efficient use of fuel thus allowing for much longer deployment times for each vessel.

In the future, we will consider the design of controllers unique to the noise characteristics of the system as well as the underlying vector field. One of the results in this study was the identification of a most-likely path to switch between basins of attraction; this path is of critical importance as shown in the simulation-generated pdf of transitioning trajectories. While the controller we employed did not explicitly make use of this path, we aim to replace it with one that does—in particular, exerting significant control effort when it is clear that a transition is likely to occur, but remaining nearly dormant when a transition is unlikely.

6 Acknowledgements

This research was performed while CRH held a National Research Council Research Associateship Award at the U.S. Naval Research Laboratory. This research is funded by the Office of Naval Research contract F1ATA01098G001, Naval Research Base Program Contract N0001412WX30002, and NSF grant IIS-1253917.

References

- [1] Forgoston, E., Billings, L., Yecko, P., and Schwartz, I. B., 2011. “Set-based corral control in stochastic dynamical systems: Making almost invariant sets more invariant”. *Chaos: An Interdisciplinary Journal of Non-linear Science*, **21**(1), pp. 013116–013116.
- [2] Mallory, K., Hsieh, M. A., Forgoston, E., and Schwartz, I. B., 2013. “Distributed allocation of mobile sensing swarms in gyre flows”. *arXiv preprint arXiv:1303.0704*.
- [3] Doostan, A., Ghanem, R. G., and Red-Horse, J., 2007. “Stochastic model reduction for chaos representations”. *Comput. Methods Appl. Mech. Engrg.*, **196**, pp. 3951–3966.
- [4] Forgoston, E., Billings, L., and Schwartz, I. B., 2009. “Accurate time series prediction in reduced stochastic epidemic models”. *Chaos*, **19**, p. 043110.
- [5] Venturi, D., Wan, X., and Karniadakis, G. E., 2008. “Stochastic low-dimensional modelling of a random laminar wake past a circular cylinder”. *J. Fluid Mech.*, **606**, pp. 339–367.
- [6] Fyrenius, A., Wigström, L., Ebbers, T., Karlsson, M., Engvall, J., and Bolger, A. F., 2001. “Three dimensional flow in the human left atrium”. *Heart*, **86**, pp. 448–455.
- [7] Provenzale, A., 1999. “Transport by coherent barotropic vortices”. *Ann Rev Fluid Mech*, **31**, pp. 55–93.
- [8] Haller, G., 2001. “Distinguished material surfaces and coherent structures in three-dimensional fluid flows”. *Physica D*, **149**, pp. 248–277.
- [9] Haller, G., 2002. “Lagrangian coherent structures from approximate velocity data”. *Phys. Fluids*, **14**(6), pp. 1851–1861.
- [10] Lekien, F., Shadden, S. C., and Marsden, J. E., 2007. “Lagrangian coherent structures in n -dimensional systems”. *J. Math. Phys.*, **48**, p. 065404.
- [11] Inanc, T., Shadden, S. C., and Marsden, J. E., 2005. “Optimal trajectory generation in ocean flows”. *Am. Auto. Cont. Council*, pp. 674–679.
- [12] Shadden, S. C., Lekien, F., and Marsden, J. E., 2005. “Definition and properties of Lagrangian coherent structures from finite-time Lyapunov exponents in two-dimensional aperiodic flows”. *Physica D*, **212**, pp. 271–304.
- [13] Bollt, E. M., Billings, L., and Schwartz, I. B., 2002. “A manifold independent approach to understanding transport in stochastic dynamical systems”. *Physica D*, **173**, pp. 153–177.

- [14] Billings, L., and Schwartz, I. B., 2008. “Identifying almost invariant sets in stochastic dynamical systems”. *Chaos*, **18**, p. 023122.
- [15] Froyland, G., and Dellnitz, M., 2003. “Detecting and locating near-optimal almost-invariant sets and cycles”. *SIAM J. Sci. Comput.*, **24**, pp. 1839–1863.
- [16] Froyland, G., and Padberg, K., 2009. “Almost-invariant sets and invariant manifolds – connecting probabilistic and geometric descriptions of coherent structures in flows”. *Physica D*, **238**, pp. 1507–1523.
- [17] Froyland, G., 2005. “Statistically optimal almost-invariant sets”. *Physica D*, **200**, pp. 205–219.
- [18] Chan, H. B., Dykman, M. I., and Stambaugh, C., 2008. “Switching-path distribution in multidimensional systems”. *Physical Review E*, **78**, p. Art. no. 051109.
- [19] Dykman, M. I., 1990. “Large fluctuations and fluctuational transitions in systems driven by coloured gaussian noise: A high-frequency noise”. *Phys. Rev. A*, **42**, pp. 2020–2029.
- [20] Dykman, M. I., McClintock, P. V. E., Smelyanski, V. N., Stein, N. D., and Stocks, N. G., 1992. “Optimal paths and the prehistory problem for large fluctuations in noise-driven systems”. *Phys. Rev. Lett.*, **68**, pp. 2718–2721.
- [21] Millonas, M., ed., 1996. *Fluctuations and Order: The New Synthesis*. Springer-Verlag.
- [22] Luchinsky, D. G., McClintock, P. V. E., and Dykman, M. I., 1998. “Analogue studies of nonlinear systems”. *Rep. Prog. Phys.*, **61**, pp. 889–997.
- [23] Billings, L., Bollt, E. M., and Schwartz, I. B., 2002. “Phase-space transport of stochastic chaos in population dynamics of virus spread”. *Phys. Rev. Lett.*, **88**, p. 234101.
- [24] Feynman, R. P., and Hibbs, A. R., 1965. *Quantum Mechanics and Path Integrals*. McGraw-Hill, Inc.
- [25] Freidlin, M. I., and Wentzell, A. D., 1984. *Random Perturbations of Dynamical Systems*. Springer-Verlag.
- [26] Wentzell, A., 1976. “Rough limit theorems on large deviations for Markov stochastic processes, I”. *Theor. Probab. Appl.*, **21**, pp. 227–242.
- [27] Hu, G., 1987. “Stationary solution of master-equations in the large-system-size limit”. *Phys. Rev. A*, **36**(12), Dec., pp. 5782–5790.
- [28] Dykman, M. I., Mori, E., Ross, J., and Hunt, P. M., 1994. “Large fluctuations and optimal paths in chemical-kinetics”. *J. Chem. Phys.*, **100**(8), pp. 5735–5750.
- [29] Graham, R., and Tél, T., 1984. “Existence of a potential for dissipative dynamical systems”. *Phys. Rev. Lett.*, **52**(1), Jan, pp. 9–12.
- [30] Maier, R. S., and Stein, D. L., 1993. “Escape problem for irreversible systems”. *Phys. Rev. E*, **48**(2), Aug, pp. 931–938.
- [31] Hamm, A., Tél, T., and Graham, R., 1994. “Noise-induced attractor explosions near tangent bifurcations”. *Physics Letters A*, **185**(3), pp. 313–320.
- [32] Mallory, K., Hsieh, M. A., Forgoston, E., and Schwartz, I. B., 2013. “Distributed allocation of mobile sensing swarms in gyre flows”. *Nonlin. Processes Geophys.*, **20**, pp. 657–668.
- [33] Yang, H., and Liu, Z., 1994. “Chaotic transport in a double gyre ocean”. *Geophys. Rev. Lett.*, **21**, p. 545.
- [34] Rom-Kedar, V., Leonard, A., and Wiggins, S., 1990. “An analytical study of transport mixing and chaos in an unsteady vortical flow”. *J. Fluid Mech.*, **214**, pp. 347–394.
- [35] Schwartz, I. B., Billings, L., Dykman, M., and Landsman, A., 2009. “Predicting extinction rates in stochastic epidemic models”. *J. Stat. Mech.-Theory E*, p. P01005.
- [36] Lindley, B. S., and Schwartz, I. B., 2013. “An iterative action minimizing method for computing optimal paths in stochastic dynamical systems”. *Physica D*, **255**, pp. 22–30.
- [37] Doedel, E. J., Champneys, A. R., Dercole, F., Fairgrieve, T., Kuznetsov, Y., Oldeman, B., Paffenroth, R., Sandstede, B., Wang, X., and Zhang, C., 2008. *AUTO-07P: Continuation and Bifurcation Software for Ordinary Differential Equations*, Feb.
- [38] Bryson, J. A. E., and Ho, Y.-C., 1975. *Applied Optimal Control: Optimization, Estimation and Control*. Taylor and Francis.
- [39] Gardiner, C. W., 2004. *Handbook of Stochastic Methods for Physics, Chemistry and the Natural Sciences*. Springer-Verlag.